

Modelling and Simulation of a Hybrid Solid Oxide Fuel Cell Coupled with a Gas Turbine Power Plant*

Valentina Amati¹, Enrico Sciubba¹, Claudia Toro^{1,**}, and Luca Andreassi²

¹Dept. of Mechanical & Aeronautical Engineering,
University of Roma "Sapienza"

Via Eudossiana 18, 00184, Roma, Italy

**E-mail: claudia.toro@uniroma1.it

²University of Roma "Tor Vergata"

Dept. of Mechanical Engineering

Via del Politecnico 1, 00133 Roma, Italy

Abstract

The paper presents a simulation of a hybrid solid oxide fuel cell-gas turbine (SOFC-GT) power generation system fueled by natural gas. In the system considered, the unreacted fuel from a topping solid oxide fuel cell is burnt in an afterburner to feed a bottoming gas turbine and produce additional power. Combustion gas expands in the gas turbine after having preheated the inlet air and fuel and it is used to generate steam required by the reforming reactions. A novel thermodynamic model has been developed for the fuel cell and implemented into the library of a modular object-oriented Process Simulator, CAMELPro™. The relevant plant performance indicators have been analyzed to evaluate the incremental increase in efficiency brought about by the introduction of the gas turbine and heat regeneration system. Simulations were performed for different values of the main plant parameters.

Keywords: Solid oxide fuel cells, combined cycles, process modeling, numerical simulation.

1. Introduction

Hybrid solid oxide fuel cell-gas turbine power generation systems represent a promising alternative energy conversion technology because of the high SOFC operating temperatures (600–1000°C) (Zhang et al., 2007).

In the system analyzed in this paper, unreacted fuel from a topping solid oxide fuel cell (FC) is burnt in an afterburner to feed a bottoming heat engine. The integration of a gas turbine looks like a natural evolution of a pressurized high temperature fuel cell system, because the gas turbine compressor can feed the FC and the cell exhaust can be easily channeled to the turbine to generate additional power (Park et al., 2007).

In addition to their high power density and rather high electrical efficiency, these systems boast a low environmental impact, enhanced by the electrochemical oxidation of the fuel. In such a combined SOFC/GT system, the gas turbine typically contributes about 1/3 of the total power output. Significant advancements in SOFC-related research and applications have been made under the pressure of a strongly growing market for distributed power generation and for small to medium scale CHP plants. However, fundamental problems such as final FC cost under market conditions and durability of FC stacks still need to be solved. The increasing interest in such applications is reflected in a large number of publications that address the so-called "configuration problem", i.e., the identification of the most convenient coupling of the SOFC process parameters with those of the GT.

The problem obviously can be formulated as an optimization under several -possibly concurrent- objective functions (higher efficiency, lower installation cost, lower environmental impact, lower cost of the kWh), but a

comprehensive cycle analysis represents a fundamental step in this kind of studies (Massardo and Lubelli, 2000; Rao and Samuelsen, 2002). Examples include parametric design analysis (Bohn et al., 2002; Campanari, 2004) hybrid systems based on an internal reforming SOFC stack (Chan et al., 2004) - an analysis of the different characteristics of internal and external reforming is reported in Liese and Gemmen (2003) - and comparisons between pressurized and atmospheric hybrid systems. It is worth mentioning that the recirculation of a portion of the SOFC exhaust to preheat the inlet air leads to an important efficiency increase (Williams et al., 2001).

The complexity of SOFC/GT systems requires reliable component models and efficient computational tools to evaluate and optimize their performance. The aim of this study is to simulate the thermodynamic process enacted by a pressurized SOFC hybrid system and conduct a sensitivity analysis of its performance based on the variation of its most relevant process parameters. This analysis, performed by means of a zero-dimensional and stationary numerical model, is particularly focused on the effects of oxygen utilization and fuel cell load on the process efficiency.

2. The Process Simulator

As a first step, a modular model of the SOFC sub-unit (composed by the SOFC itself and by its pre-reformer) has been implemented and integrated in an existing process simulator, CAMEL-Pro™ (Falcetta and Sciubba, 1996; www.turbomachinery.it, 2008). CAMEL-Pro™ is written in C++ and C#, is based on a completely and genuinely object-oriented approach, and is equipped with a user-friendly graphical interface that allows for the simulation

*This paper is an updated version of a paper published in the ECOS08 proceedings. It is printed here with permission of the authors and organizers.

**Corresponding Author

and analysis of several energy conversion processes. The system is represented as a network of components connected by material and energy streams; each component is characterized by a set of equations describing the thermodynamic changes imposed on the streams; in mathematical terms, this equation system is not closed, and, therefore, needs a proper number of boundary conditions in terms of known flow parameters. In practical terms, this means that the computed solution depends on both the plant configuration and on the assigned boundary conditions.

An optimized iterative Newton-Raphson algorithm is used to solve the global equation system. The main feature of CAMEL-Pro™ is in fact its modularity that enables users to expand the code by adding new components or by modifying the model of the existing ones. We exploited these capabilities to introduce the proper process equations for the SOFC group model. In the gas model adopted in CAMEL-Pro™, the specific heat is calculated by a fifth order polynomial in temperature (Lanzafame and Messina, 2000), and enthalpy and entropy are obtained by exact integration of these polynomials. The gas constant R is calculated according to the mixture rule. For water/steam properties, CAMEL-Pro™ uses the IAPWS library (The International Association for the Properties of Water and Steam, 1997). Other models for material streams are also available (Colonna et al., 2004).

3. The Model of the SOFC Sub-Unit

SOFC power systems consist of a stack in which individual cells are modularly assembled with proper electrical connections into units with the desired output capacity, and by auxiliary components, whose arrangement strongly depends on fuel cell type, fuel physical properties, and on the particular application. For the purpose of the present study, the system (Figure 2) consists of:

- 1) A fuel processing sub-system. The sub-system is designed to produce a suitable fuel for SOFC operation. It consists of a reformer or gasifier that transforms the "raw" fuel (a hydrocarbon) into a H₂-rich syngas and other devices for the removal of impurities (such as the desulphurizer, not included in the present study) and for thermal conditioning.
- 2) A heat management sub-system. It manages the thermal flows throughout the system and monitors the stack thermal level, acting on it through the mass flowrate of the cathodic cooling air.
- 3) A water management sub-system. Water injection is crucial in some components. At the reformer inlet, water promotes and maintains the steam reforming reaction; at the cell inlet, it reduces the risks of carbon deposition.
- 4) An electric power conditioning sub-system. Since fuel cell stacks provide a variable DC voltage output that is not suitable to drive an external load, electric power conditioning is typically required.

The model discussed and implemented here is based on energy and mass balances coupled with appropriate expressions for the reactions kinetics, thermodynamic constants and material properties. The balance equations are written as macroscopic balances, in the form of finite equations: this is a "First Law" approach, since these equations simply express the inlet/outlet mass and energy balances for each component of the SOFC sub-unit. The

exergy analysis is the topic of a separate paper (Amati et al., 2008).

The following assumptions were made:

- Steady state conditions,
- All external walls of all components of the SOFC sub-unit are adiabatic,
- The shift reaction is at equilibrium both in the reformer and in the SOFC stack,
- The fuel is completely sulphur free,
- The reforming reaction is completely developed in the SOFC while the percentage of methane which reacts in the reformer is treated as an input variable,
- The pressure drop within the cell channels and within the reformer is neglected,
- The reformer outlet gas temperature is equal to the reformer process temperature,

3.1 Reformer Model

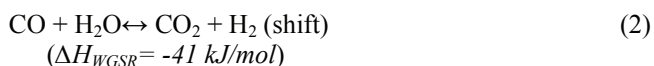
To run a FC, natural gas must be converted into hydrogen. This transformation is partially carried out in an external reactor called the Pre-reformer, and then it continues (in a molar sense) within the fuel cell that is therefore properly given the attribute of "internally reforming FC".

A model of the pre-reformer must account for the rather complex set of chemical reactions taking place in this component. Since modeling all of the reactions is quite complex (see for example, Xu and Froment, 1989), usually only methane steam reforming and water gas shift are considered:

Reforming reaction:



Water gas shift reaction:



The sensible heat of the reactants provides the required activation energy. The reactants are methane (at 1035 K) and steam (at 415 K) which are supplied to the reformer respectively from the fuel compressor and from the recycled flow deriving from the water-rich anodic exhaust of the SOFC.

However, other undesired reactions might occur simultaneously with (1) and (2). The most dangerous is the so-called carbon deposition (3). In systems that use biomass as fuel, the syngas generated in the biomass gasifier could contain considerable amounts of tars: this is unacceptable here, because tar can lead to the deposition of atomic carbon at the SOFC anode, thus effectively poisoning the cell. Other dominant reactions are the Boudouard reaction (4), and CO hydrogenation (5).



The carbon formation and deposition (3) can be avoided working locally with an excess of steam. It is therefore

important to maintain a Steam-to-Carbon (SC) ratio higher than 2. In the present work the carbon deposition phenomenon is neglected because a Steam-to-Carbon ratio higher than 2 has been considered.

Furthermore, by considering moist hydrogen as the FC fuel it is possible to neglect the Boudouard reaction (4). In the same line of reasoning, also the CO hydrogenation (5) is neglected since it displays a much lower reaction rate with respect to the CO-shift (2). The value of the percentage of methane which reacts in the reformer (Eq (1)) must be assigned by the user.

The shift reaction is considered to reach thermodynamic equilibrium, with an equilibrium constant given by (Bustamante, 2004):

$$K_{eq} = e^{\left(-4,33 + \frac{4577,8}{T}\right)} \quad (6)$$

where:

$$K_{eq} = \frac{P_{CO_2} \cdot P_{H_2}}{P_{CO} \cdot P_{H_2O}} \quad (7)$$

in which the partial pressures are calculated at the reformer outlet temperature.

The above equations can be used to calculate the moles of CO ($x_{CO,WGSR}$) that react in reaction (2). Equations (8) and (9) express the mass and energy balances for the reformer. Equation (9) includes, in addition to the input and output energy terms, both an "internal consumption term" ($\Delta H_{Ref} \cdot x_{CH_4,Ref}$) that accounts for the endothermality of the reforming reaction and an "internal generation term" that accounts for the exothermality of the shift reaction ($\Delta H_{WGSR} \cdot x_{CO,WGSR}$). Moreover, it includes the endothermic heat Q_{ext} added to the reformer to maintain the operating temperature.

$$\left\{ \begin{array}{l} CH_4^o = CH_4^i - x_{CH_4,Ref} \\ CO^o = CO_i + x_{CH_4,Ref} - x_{CO,WGSR} \\ CO_2^o = CO_2^i + x_{CO,WGSR} \\ H_2^o = H_2^i + 3x_{CH_4,Ref} + x_{CO,WGSR} \\ H_2O^o = H_2O^i - x_{CH_4,Ref} - x_{CO,WGSR} \end{array} \right. \quad (8)$$

$$\begin{aligned} \dot{m}_{i,Ref} \cdot h_{i,Ref} + Q_{Ref} + Q_{ext} &= \dot{m}_{o,Ref} \cdot h_{o,Ref} + Q_{WGSR} \\ Q_{Ref} &= \left| \Delta H_{Ref} \cdot x_{CH_4,Ref} \right| \\ Q_{WGSR} &= \left| \Delta H_{WGSR} \cdot x_{CO,WGSR} \right| \end{aligned} \quad (9)$$

3.2 SOFC Model

In addition to the reforming (1) and the shift (2) reactions, it is necessary to account for the electrochemical oxidation of the hydrogen inside of the FC:



The fuel is completely reformed inside the cell, and the mole fraction of methane ($x_{CH_4,Ref}$), participating in reaction (1) is equal to the mole fraction of methane entering the fuel cell: $x_{CH_4,Ref} = CH_4^i$.

Since the shift reaction in the FC is also considered to reach thermodynamic equilibrium, the concentration of each species after the water-shift reaction is controlled by the equilibrium constant (6).

A new variable is commonly used in the evaluation of FC performance: the fuel utilization factor, defined as:

$$U_f = \frac{z}{(H_2^i + CO^i + 4CH_4^i)} \quad (11)$$

where each mole of CH_4 generates 4 moles of H_2 (3 by reforming and 1 by shift). The variable z is the number of H_2 moles reacting in Equation (10).

In the evaluation of fuel cell performance, U_f is assigned. By using Equation (11) it is, therefore, possible to calculate z and to obtain the electrical current of the cell:

$$I_{TOT} = z \cdot 2 \cdot F \quad (12)$$

Thus, in the mass balances (13), both chemical and electro-chemical reactions are included.

$$\left\{ \begin{array}{l} CH_4^o = CH_4^i - x_{CH_4,Ref} \\ CO^o = CO_i + x_{CH_4,Ref} - x_{CO,WGSR} \\ CO_2^o = CO_2^i + x_{CO,WGSR} \\ H_2^o = H_2^i + 3x_{CH_4,Ref} + x_{CO,WGSR} - z \\ H_2O^o = H_2O^i - x_{CH_4,Ref} - x_{CO,WGSR} + z \end{array} \right. \quad (13)$$

In a SOFC stack, the calculation of the electrical current-voltage characteristic curve starts with the evaluation of the cell open circuit potential (ideal Nernst potential):

$$V_{id} = E^0_{H_2} + \frac{RT}{2F} \ln \left(\frac{P_{H_2} \cdot P_{O_2}^{0.5}}{P_{H_2O}} \right) \quad (14)$$

where $E^0 = 1.272 - 2.764 \cdot 10^{-4} T_c$ is the ideal voltage for hydrogen oxidization at ambient pressure, and is a function of cell temperature (Campanari and Iora, 2004).

Since the cell voltage decreases from the inlet to the outlet because of the ongoing change in the partial pressures of the participating chemical species, the FC open-circuit potential was assumed to be the arithmetic average between the inlet ($V_{i,id}$) and the outlet ($V_{o,id}$) voltage.

The Nernst potential is reduced when the electrical cell circuit is closed, because of the irreversibilities introduced by the ohmic resistance of the cell elements, by the activation barriers at the electrodes and by the concentration polarization losses.

Thus, the cell voltage is calculated as:

$$V_{Cell} = V_{id} - \Delta V_{act} - \Delta V_{ohm} - \Delta V_{conc} \quad (15)$$

The ohmic overvoltages are expressed by the Ohm law:

$$\Delta V_{ohm} = I \cdot \left(\frac{\rho_{an} \cdot \tau_{an}}{A_{act}} + \frac{\rho_{cat} \cdot \tau_{cat}}{A_{act}} + \frac{\rho_{el} \cdot \tau_{el}}{A_{act}} + \frac{\rho_{int} \cdot \tau}{A_{act}} \right) \quad (16)$$

where A_i represents the active area of the i^{th} element, τ_i is the elements thickness and ρ_i is the corresponding material resistivity, calculated with a temperature-dependent relation (Colonna and van der Stelt, 2004). Diffusion “blockages” at the anode and cathode have been included in the evaluation of the concentration overpotential. They are given by (Van Herle et al., 2004):

$$\Delta V_{conc_{an}} = \frac{RT}{2F} \ln(1 - U_f) \quad (17)$$

$$\Delta V_{conc_{cat}} = \frac{RT}{2F} \ln(1 - U_f \cdot U_a) \quad (18)$$

where U_a is the oxygen utilization factor.

Whereas this description may oversimplify the diffusion process at the FC electrodes, it has the advantage of correctly reproducing the experimentally observed decreasing current–voltage (I–V) FC at high fuel utilisations.

Activation polarisation is related to the intrinsic irreversibility of the electrochemical reaction. The activation polarizations ΔV_{act} are expressed in implicit form by the Butler–Volmer equation (Costamagna et al., 2004):

$$j = j_0 \left[\exp\left(\alpha \frac{n_e F}{RT} \Delta V_{act}\right) - \exp\left(- (1 - \alpha) \frac{n_e F}{RT} \Delta V_{act}\right) \right] \quad (19)$$

where j_0 is the exchange current density and α the apparent charge transfer-coefficient. Eq. (19) applies to both anode and cathode; under open circuit conditions, direct and reverse electrochemical reactions occur simultaneously at each electrode, and are both equal to the exchange current density j_0 which can be expressed as a function of the Arrhenius law and of the composition of the reacting gases (Costamagna et al., 2004):

$$j_{0,Cat} = \gamma_C \left(\frac{p_{O_2}}{p_{ref}} \right)^{0.25} \exp\left(- \frac{E_{act,C}}{RT}\right) \quad (20)$$

$$j_{0,An} = \gamma_A \left(\frac{p_{H_2}}{p_{ref}} \right) \left(\frac{p_{H_2O}}{p_{ref}} \right)^{-0.5} \exp\left(- \frac{E_{act,A}}{RT}\right) \quad (21)$$

Again, the arithmetic average of the species concentration between the inlet and the outlet was used to calculate the anode and cathode exchange current density.

The energy balance (Eq. 22) includes the electrical power W_{el} and the enthalpy changes of the chemical (ΔH_{Ref} and ΔH_{WGSR}) and electrochemical (ΔH_{ox}) reactions, and can be used to evaluate the oxygen utilization U_a (i.e. the air inlet molar flow) if an acceptable temperature at the cell outlet is specified.

$$\begin{aligned} \dot{m}_{Fuel}^i \cdot h_{Fuel}^i + \dot{m}_{Air}^i \cdot h_{Air}^i + Q_{Ref} &= \\ Q_{WGSR} + Q_{ox} + W_{el} + \dot{m}_{Fuel}^o \cdot h_{Fuel}^o + \dot{m}_{Air}^o \cdot h_{Air}^o & \\ Q_{Ref} &= \left| \Delta H_{Ref} \cdot x_{CH_4,Ref} \right| & (22) \\ Q_{WGSR} &= \left| \Delta H_{WGSR} \cdot x_{CO,WGSR} \right| \\ Q_{ox} &= \left| \Delta H_{Ox} \cdot z \right| \end{aligned}$$

The oxygen moles consumed in reactions (10) are $z/2$ according with the stoichiometric coefficients of the reaction. Thus, the air utilization factor is defined as:

$$U_a = \frac{z}{O_2^i} \quad (23)$$

3.3 Model Validation: Reference SOFC

A planar SOFC proposed as a benchmark case by the International Energy Agency (IEA) is analyzed in this study (Achenbach, 1994&1996). The FC output power is:

$$W_{El} = V_C \cdot I_{TOT} \quad (24)$$

The SOFC electric generation efficiency is then calculated as:

$$\eta_{SOFC} = \frac{W_{el}}{\left(CH_4^i \cdot LHV_{CH_4} + CO^i \cdot LHV_{CO} + H_2^i \cdot LHV_{H_2} \right)} \quad (25)$$

The results of the simulation, considering the operating conditions summarized in Table 1, are in good agreement with Achenbach (1994). In fact, the calculated cell voltage of 0.647 V falls within the reference limits of 0.649V–0.633V (Achenbach, 1994).

Table 1. SOFC Operating Conditions.

Operating Conditions	
Pressure	101.325 Pa
T_{in} (fuel)	1173 K
T_{in} (air)	1173 K
U_a	0.14
U_f	0.85
Mean current density	3000 A/m ²
% pre-ref.	30%
SC Ratio	2.5

The polarization curve and the electrical efficiency obtained for the simulated SOFC system are shown in Figure 1 for different current densities. Thus for the simulated SOFC a peak efficiency of 47% for a current density of 3000 A/m² and U_f of 85% is observed at ambient pressure.

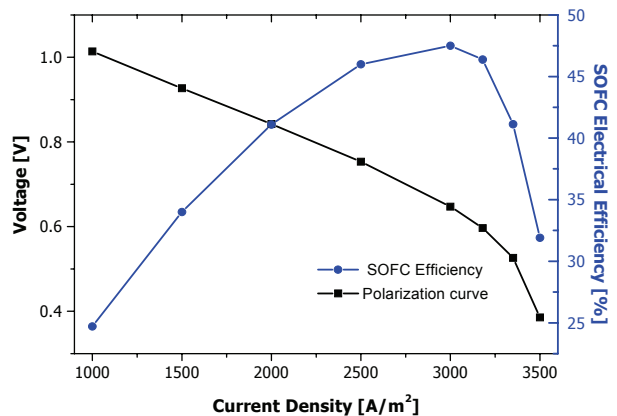


Figure 1. Polarization Curve and SOFC Efficiency.

4. System Level Simulation of the SOFC/GT Hybrid System

4.1 Plant Flowsheet

Figure 2 shows the flowsheet of the SOFC/GT hybrid system simulated with CAMEL-Pro™. External pre-filtered input air (Stream 27) is first compressed in the main process compressor (C_{air}) and then preheated by the turbine exhaust gas in a gas/gas heat exchanger (AHR2). The pre-heated air is further reheated in a high-temperature recuperative heat exchanger (AHR3). The fuel (natural gas, Stream 29) is compressed in the fuel compressor (C_{fuel}) and then pre-heated and humidified by steam injection in the heat exchanger (AHR1). The required steam (Stream 4) is generated in a heat recovery Boiler (RB) fed by the gas turbine exhaust. The compressed and pre-heated fuel stream is then mixed with the steam-rich anodic recirculated stream.

Since the adopted model prescribes the SC Ratio to be an input parameter, the required water flow is calculated taking into account also the steam content of the recirculated flow. Methane is partially reformed in the pre-reformer and the residual CH_4 is internally reformed at the SOFC anode. An external heat supply is required by the Reformer to maintain the desired operating temperature (Stream 3).

The air and the pre-reformed fuel enter the SOFC where the electrochemical reaction (10) takes place. Part of the anode exhaust gas is recirculated to the pre-reformer inlet (Stream 12). To reach the desired turbine inlet temperature, part of the fuel at the compressor outlet (Stream 14) bypasses the SOFC group, is mixed with the remaining anode exhaust gas (Stream 13) and enters the combustion chamber (Stream 15). After the combustion, part of the high temperature outlet gas (Stream 19) is directed to the recuperative heat exchanger (AHR3) to reheat the air entering the SOFC. Downstream of AHR3 this stream is remixed with the SOFC exhaust and enters the turbine (TB). The turbine exhaust gas is used to preheat air (AHR2), fuel (AHR1) and the feed-water (RB). The temperature of both the air and fuel exiting the SOFC is controlled by throttling the inlet air flow.

4.2 Steady-State Simulation

The above described model has been implemented in the CAMEL-Pro™ simulator to perform a steady-state calculation of the SOFC/GT process. Pipe friction losses have been neglected in the present study.

The design-point parameters are reported in Table 2, while Tables 3 and 4 present the calculated results. The simulation shows that the anodic mass flow rate (Stream 5 in Figure 2) increases as the flow passes through fuel cell, while the mass flow on the cathodic side decreases (Streams 8-9) due to reaction (10) occurring within the SOFC.

It can be seen that with a S/C of 2.5 and a percentage of anodic recirculation of 35% the amount of water vapor added is about 0.03 kg/s. To maintain the design TIT at 1250 K, it is necessary to inject about 28% of the fuel at the compressor outlet (stream 14) directly into the combustion chamber. The exhaust gas from the system (Stream 36) is composed of Nitrogen (73.4%), steam (6.4%), Oxygen (15.9%) and CO_2 (4.3%). The power outputs of the system are reported in Table 3, together with the power needed by

Table 2 Parameters Assumed at Design Conditions.

SYSTEM PARAMETERS	
COMPRESSOR	
Isentropic efficiency	85%
Inlet Pressure	101.325 Pa
Inlet Temperature	298 K
Pressure ratio	11
TURBINE	
Isentropic efficiency	85%
Inlet Temperature, TIT	1250 K
Expansion ratio	9.7
SOFC	
Fuel Utilization	85%
Oxygen Utilization	20%
Current density	3800 Am^{-2}
Number of cells	32100
Inlet temperature	1173 K
REFORMER	
S/C Ratio	2.5
Operating temperature	1173 K
Heat exchange efficiency	0.85

the air and fuel compressors, the pump and the thermal power required by the pre-reformer.

$$\eta_{SOFC/GT} = \frac{P_{Tot}}{m_{Fuel} \cdot LHV_{Fuel} + Q_{Ref}} \quad (26)$$

From Tables 3 and 4, Eq. (26) provides a value of 0.593 for the efficiency of the SOFC/GT system. The electrical efficiency of the cell as a stand-alone is 53%. This demonstrates that the introduction of the bottoming TG cycle increases the electrical efficiency, first because it recovers a portion of the high pressure energy of the gas exhausted from the SOFC and uses it to pressurize the SOFC inlet air. Moreover, the high temperature exhaust heat obtained simultaneously with power generation is used in fuel reforming and in the regenerative pre-heating of fuel and air.

Table 3. Power Flows Within the System.

SOFC Electric Power			
Id	Power	Current	Voltage
	kW	A	V
10	875	1217090	0.719
Shaft Power			
	Id	kW	
TG	23	1240.8	
Cair	26	760	
Cfuel	28	24.97	
Pump	33	0.041	
Ref. Heat	3	279	

4.3 System Performance Under Variable Operating Pressure and Turbine Inlet Temperature

The results obtained by changing both compressor pressure ratio and turbine inlet temperature are shown in Figure 3. The system efficiency increases from $\beta=3$ to $\beta=11$, where it peaks, and then decreases slightly. This behavior can be explained by considering that overpotentials are positively affected by gas pressures and

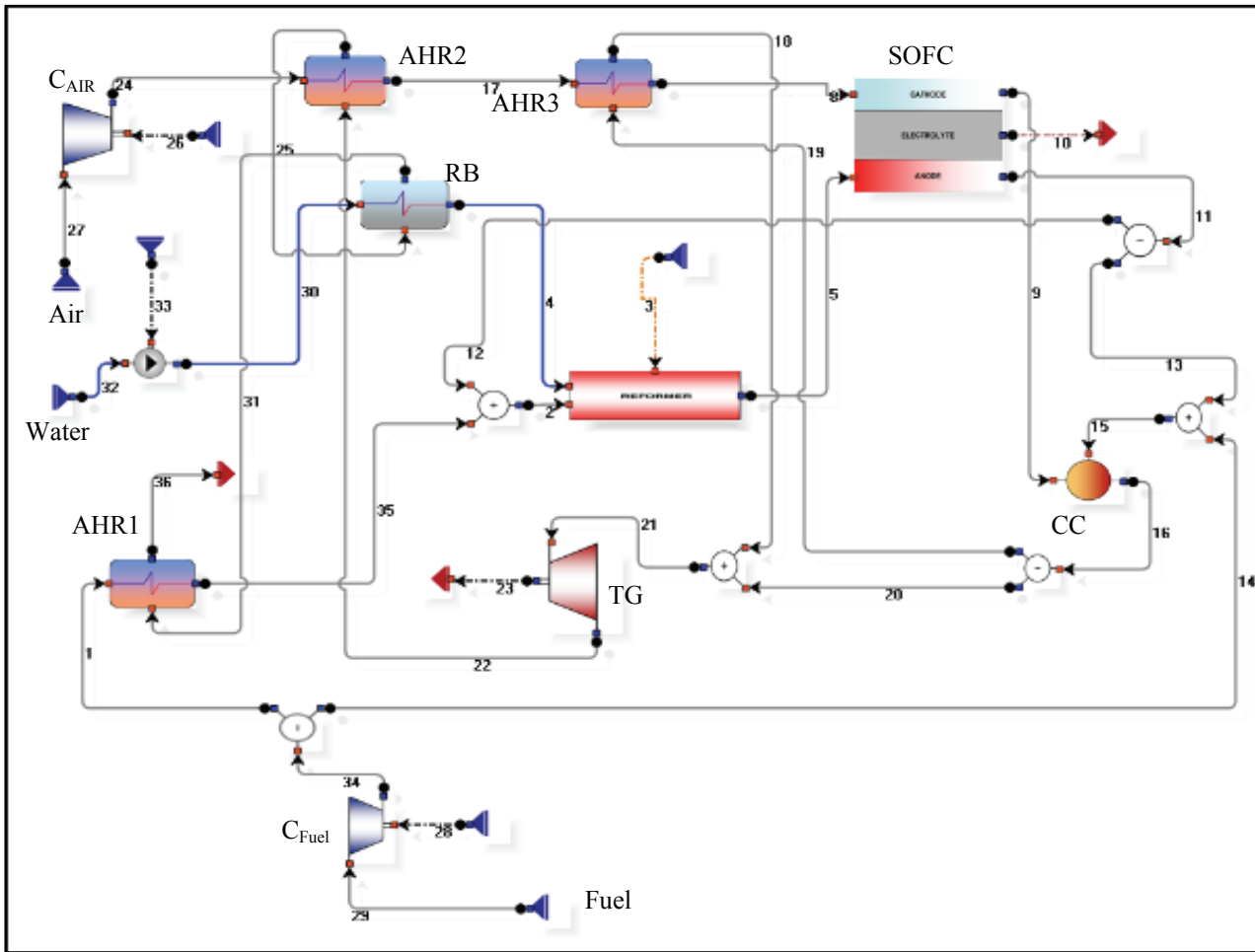


Figure 2. CAMEL-Pro™ Flow Sheet of the SOFC/GT Hybrid System.

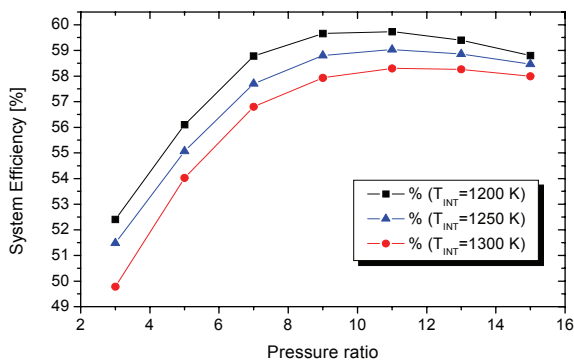


Figure 3. System Performance with Variable SOFC Pressure and Turbine Inlet Temperature.

the cell performance at 1000°C is well approximated by the semi-empirical relation (Hirchenhofer, 2000).

$$\Delta V_p (mV) = 59 \log \frac{p_2}{p_1} \quad (27)$$

where p_1 and p_2 are cell operating pressures. The overall system efficiency decreases with the TIT because as the net power output from the GT increases, so does its contribution to the overall power output. Since the gas

turbine is less efficient than the fuel cell, the weighed overall system efficiency is negatively affected (of course, the specific work increases, and therefore there may be an advantage to build real systems with a higher-than optimal TIT gas turbine).

4.4 System Performance Under Variable SOFC Load and Oxygen Utilization.

The effect of a variable load is studied with variable current density and under the assumptions reported in Table 2 (most notably, under constant $U_f = 85\%$). Figure 4 shows the dependence of the efficiency on the current density. Both SOFC and system efficiency display a negative trend with respect to current density, SOFC efficiency decreasing sooner than system efficiency. The effect of oxygen utilization was studied under the assumption of a constant fuel utilization factor.

As previous explained, Figure 1 represents the polarization curve and the efficiency profile for the SOFC increasing current density considering a variable utilization factor U_f . On the other hand, Figure 4 represents the SOFC and system efficiency evaluated considering a constant U_f value. Therefore, it is obtained increasing the fuel flow rate. Increasing the fuel flow rate causes the decreasing of the cell voltage (due to an increasing of cell overpotentials) and does not compensate for the increase in current density. Accordingly, the SOFC efficiency gradually decreases.

Table 4: Properties and % Composition of Material Flows in the SOFC/GT Cycle.

Id	m	p	T	h	s	ex	xO2	xN2	xCO2	xH2O	xH2	xCH4	xCO	LHV
	kg/s	kPa	K	kJ/kg	kJ/(kg K)	kJ/kg	kg/kg	kg/kg	kg/kg	kg/kg	kg/kg	kg/kg	kg/kg	kJ/kg
1	0.028	1114	522	621	13.06	50704	-	-	-	-	-	100%	-	50100
2	0.118	1080	1036	2588.9	10.05	14343	5.5%	-	31.9%	40.7%	0.46%	23.8%	3.13%	12788
4	0.031	1092	415	493	1.75	250.9	-	-	-	100%	-	-	-	-
5	0.149	1080	1173	3024	7.58	3135	-	-	37.9%	42.6%	2.7%	14.2%	2.7%	10635
8	2.166	1070	1173	964.5	7.73	732.4	23%	75.76%	0.05%	1.2%	-	-	-	-
9	2.072	1070	1257	1052.5	7.71	802.6	19.5%	80.17%	0.05%	1.2%	-	-	-	-
11	0.250	1080	1273	3122.3	9.31	3019	-	-	41.8%	53.4%	0.6%	-	4.1%	1127
12	0.090	1080	1273	3122.3	9.31	3019	-	-	41.8%	53.4%	0.6%	-	4.1%	1127
13	0.160	1080	1273	3122.3	9.31	3019	-	-	41.8%	53.4%	0.6%	-	4.1%	1127
14	0.011	1114	522	621.1	13.06	50704	-	-	-	-	-	100%	-	50100
15	0.171	1080	1220	2957.6	8.93	6179	1.5%	-	39.1%	49.9%	0.56%	6.6%	3.8%	4351
16	2.243	1070	1570	1530.1	8.37	1186	15.8%	73.44%	4.3%	6.3%	-	-	-	-
17	2.166	1092	800	532.6	7.29	431.9	23%	75.76%	0.05%	1.2%	-	-	-	-
18	1.200	1048	960	750.7	7.76	588.7	15.8%	73.44%	4.3%	6.3%	-	-	-	-
19	1.200	1070	1570	1530.1	8.37	1186	15.8%	73.44%	4.3%	6.3%	-	-	-	-
20	1.043	1070	1570	1530.1	8.37	1186	15.8%	73.44%	4.3%	6.3%	-	-	-	-
21	2.243	1048	1250	1113.1	8.08	854.5	15.8%	73.44%	4.3%	6.3%	-	-	-	-
22	2.243	108	801	559.9	8.22	260.7	15.8%	73.44%	4.3%	6.3%	-	-	-	-
24	2.166	1114	636	351.9	7.04	327.2	23%	75.76%	0.05%	1.2%	-	-	-	-
25	2.243	105	650	385.4	7.99	155.4	15.8%	73.44%	4.3%	6.3%	-	-	-	-
27	2.166	101.3	298	0.	6.96	0.	23%	75.76%	0.05%	1.2%	-	-	-	-
29	0.039	101.3	298	0.	13.27	50019.	-	-	-	-	-	100%	-	50100
30	0.031	1114	298	1.2	0.36	174.02	-	-	-	100%	-	-	-	-
31	2.243	103	644	378.7	7.99	149.9	15.8%	73.44%	4.33%	6.35%	-	-	-	-
32	0.031	101.3	298	0.	0.37	173.0	-	-	-	100%	-	-	-	-
34	0.039	1114	522	621.1	13.06	50704	-	-	-	-	-	100%	-	50100
35	0.028	1092	600	882.1	13.45	50836	-	-	-	-	-	100%	-	50100
36	2.243	101	642	375.4	7.99	146.4	15.8%	73.44%	4.33%	6.35%	-	-	-	-

Figure 5 shows the SOFC efficiency vs. the oxygen utilization. The fuel cell efficiency and the oxygen utilization reveal an opposite trend, because the average oxygen molar fraction drops with increasing oxygen utilization within the fuel cell. The effect of oxygen utilization on system performance is presented in Figure 5.

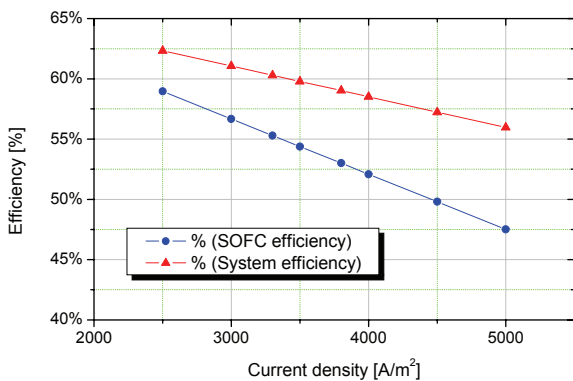


Figure 4. System Performance with Variable Fuel Cell Load.

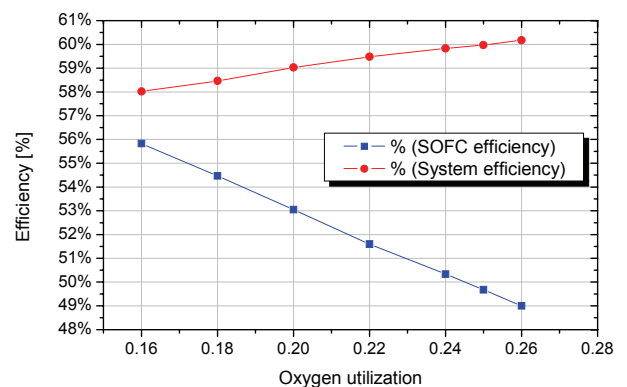


Figure 5. System Performance with Variable Oxygen Utilization.

5. Conclusions

A thermodynamic model of a natural gas-fed solid oxide fuel cell stack with internal and external reforming has been presented. Despite its relatively simple formulation (zero dimensional and stationary), the model has provided accurate and reliable results, and can therefore be regarded as a useful tool to predict the fuel cell performance.

The FC model has been integrated in a more complex SOFC/GT hybrid plant model and the overall performance

has been evaluated in order to assess the system sensitivity to variations in the main operating parameters. The efficiency of the simulated plant reaches about 59.3% at design conditions, and the analysis reveals the existence of an “optimal” pressure ratio for both SOFC efficiency and system efficiency ($\beta \approx 11$) and predicts a decrease in performance with an increasing TIT. At the level implemented here, the simulation is not computationally intensive, taking only few seconds to simulate the behavior of the whole SOFC/GT group on a commercial processor (Pentium4, 2.80 GHz).

Nomenclature

A_{act}	cell active area	[m ²]
E_{act}	activation energy	[kJ/mol]
$E_{H_2}^0$	H ₂ oxidation ideal voltage	[V]
F	Faraday's constant	[C/mol]
h	specific enthalpy	[kJ/kg]
I_{TOT}	SOFC electric current	[A]
j	cell current density	[A/m ²]
j_0	exchange current density	[A/m ²]
K_{eq}	CO-shift reaction equilibrium constant	
LHV	lower heating value	[kJ/kg]
\dot{m}	mass flow rate	[kg/s]
n_e	number of electrons participating in the electrochemical reaction	
p_i	partial pressure of component i^{th}	[Pa]
Q	heat flow	[kW]
R	universal gas constant	[kJ/(molK)]
SC	steam-to-carbon ratio	
T	temperature	[K]
U_a	oxygen utilization factor	
U_f	fuel utilization factor	
V	electric potential	[V]
W_{el}	SOFC power	[kW]
z	moles of H ₂ oxidized	[mol/s]
α	charge transfer coefficient	
β	pressure ratio	
γ	Arrhenius pre-exponential factor	[A/m ²]
ΔH_k	enthalpy change of reaction k	[kJ/mol]
ΔV	overpotential losses	[V]
ε	reformer heat exchange efficiency	
η_{SOFC}	SOFC electrical efficiency	
ρ	material resistivity	[Ωm]
τ	Thickness	[m]

Subscripts

A	anode
act	activation
C	cathode
conc	concentration
el	electrochemical reaction
ohm	ohmic
Ref	reforming reaction
WGSR	water-gas shift reaction

References

- Achenbach, E., 1994: Status of the IEA-benchmark test on stack-modelling, *IEA Workshop*, Roma, Italy.
- Achenbach, E., 1996, SOFC stack modeling, Final Report of Activity A2, Annex II: Modeling and Evaluation of Advanced Solid Oxide Fuel Cells, *IEA Programme on R, D&D on Advanced Fuel Cells*, Juelich, Germany.
- Amati V., Sciubba E., Toro C., 2008, Exergy analysis of a solid oxide fuel cell-gas turbine hybrid power plant, *ASME Paper IMECE2008-68339*.
- Bohn D., Poppe N., Lepers J, 2002, Assessment of the potential of combined micro gas turbine and high temperature fuel cell systems, *ASME Paper GT-2002-30112*.
- Bustamante F., 2004, High-Temperature Kinetics of the Homogeneous Reverse Water-Gas Shift Reaction, *AIChE Journal*, Vol. 50, No. 5, pp. 1028-1041.
- Campanari S., Iora P., 2004, Definition and sensitivity analysis of a finite volume SOFC model for a tubular cell geometry, *J. Power Sources*, Vol. 132, pp. 113-126.
- Campanari S., 2004, Parametric analysis of small scale recuperated SOFC/gas turbine cycles, *ASME Paper GT2004-53933*.
- Chan S.H., Ho H.K., Tian Y., 2002, Modelling of a simple hybrid solid oxide fuel cell-gas turbine power plant, *J. Power Sources*, Vol. 109, pp. 111-120.
- Colonna, P., van der Stelt, T. P., 2004, FluidProp a program for the estimation of thermophysical properties of fluids, Energy Technology Section, Delft University of Technology, The Netherlands.
- Costamagna P., Selimovic A., Del Borghi M., Agnew G., 2004, Electrochemical model of the integrated planar solid oxide fuel cell (IP-SOFC), *Chem. Eng. J.*, Vol. 102, pp. 61-69.
- Falcetta M., Sciubba E., 1995, A Computational Modular Approach to the Simulation of Power Plants, *ASME-AES Heat Recovery Systems & CHP*, Vol. 15, No. 2, pp. 131-145.
- Hirchenhofer J.H., 2000, *Fuel Cell Handbook, Fifth Edition*, Person Corporation, Reading, PA 19607.
- Lanzafame, R, Messina, M, 2000, A novel interpolating polynomial for the calculation of gas enthalpy, *La Termotecnica*, (in Italian).

- Liese E.A., Gemmen R.S., 2003, Performance comparison of internal reforming against external reforming in a SOFC/gas turbine hybrid system, *ASME Paper GT 2003-38566*.
- Massardo A.F., Lubelli F., 2000, Internally Reforming Solid Oxide Fuel Cell - Gas Turbine Combined Cycles (IRSOFC-GT). Part A: Cell Model and Cycle Thermodynamic Analysis, *J. Eng. Gas Turb. & Power*, Vol. 122, pp. 27-35.
- Park S.K., Oh K.S., Kim T.S., 2007, Analysis of the design of a pressurised SOFC hybrid system using a fixed gas turbine design, *J. Power Sources*, Vol. 170, pp.130-139
- Rao A.D., Samuelsen G.S., 2002, Analysis strategies for tubular solid oxide fuel cell based hybrid systems, *J. Eng. Gas Turb. & Power*, Vol. 124, pp. 503–509
- The International Association for the Properties of Water and Steam, 1997, Release on the IAPWS Industrial Formulation 1997 for the Thermodynamic Properties of Water and Steam, Erlangen, Germany.
- Van Herle J., Maréchal F., Leuenberger, S., Membrez, Y., Bucheli, O., Favrat, D., 2004, Process flow model of solid oxide fuel cell system supplied with sewage biogas, *J. Power Sources*, Vol. 131, pp.127–141.
- Williams G.J., Siddle A., Pointon K., 2001, Design optimisation of a hybrid solid oxide fuel cell & gas turbine power generation system, ALSTOM Power Techn. Centre TR, www.turbomachinery.it, 2008, CAMEL-Pro™ Users Manual, rev. 4
- Xu, J., Froment, G.F., 1989, Methane steam reforming, methanation and water-gas shift: I. Intrinsic kinetics, *AIChE Journal*, Vol. 35, pp.88-96.
- Zhang, X., Li, J., Li, G., Feng, Z., 2007, Cycle analysis of an integrated solid oxide fuel cell and recuperative gas turbine with an air reheating system, *J. Power Sources*, Vol. 164, pp. 752–760.